Augmented Biosynthesis of Cadmium Sulfide Nanoparticles by Genetically Engineered *Escherichia Coli*

Yen-Lin Chen
Food Industry Research and Development Institute, Hsinchu, Taiwan 300

Hsing-Yu Tuan, Chun-Wen Tien, and Wen-Hsin Lo
Dept. of Chemical Engineering, National Tsing Hua University, Hsinchu, Taiwan 300

Huang-Chien Liang
Biomedical Engineering Research Laboratories, Industrial Technology Research Institute, Hsinchu, Taiwan 310

Yu-Chen Hu
Dept. of Chemical Engineering, National Tsing Hua University, Hsinchu, Taiwan 300

DOI 10.1002/btpr.199
Published online July 23, 2009 in Wiley InterScience (www.interscience.wiley.com).

Microorganisms can complex and sequester heavy metals, rendering them promising living factories for nanoparticle production. Glutathione (GSH) is pivotal in cadmium sulfide (CdS) nanoparticle formation in yeasts and its synthesis necessitates two enzymes: γ-glutamylcysteine synthetase (γ-GCS) and glutathione synthetase (GS). Hereby, we constructed two recombinant E. coli *ABLE C strains to over-express either γ-GCS or GS and found that γ-GCS over-expression resulted in inclusion body formation and impaired cell physiology, whereas GS over-expression yielded abundant soluble proteins and barely impeded cell growth. Upon exposure of the recombinant cells to cadmium chloride and sodium sulfide, GS over-expression augmented GSH synthesis and ameliorated CdS nanoparticles formation. The resultant CdS nanoparticles resembled those from the wild-type cells in size (2–5 nm) and wurtzite structures, yet differed in dispersibility and elemental composition. The maximum particle yield attained in the recombinant* E. coli *was ≈2.5 times that attained in the wild-type cells and considerably exceeded that achieved in yeasts. These data implicated the potential of genetic engineering approach to enhancing CdS nanoparticle biosynthesis in bacteria. Additionally,* E. coli*-based biosynthesis offers a more energy-efficient and eco-friendly method as opposed to chemical processes requiring high temperature and toxic solvents.* © 2009 American Institute of Chemical Engineers *Biotechnol. Prog.,* 25: 1260–1266, 2009
Keywords: cadmium sulfide (CdS), genetic engineering, glutathione, glutathione synthetase, Escherichia coli*, nanoparticles*

Introduction

There is an enormous interest in the synthesis of nanomaterials, thanks to their unique optical, chemical, photoelectrochemical, and electronic properties,[1,2] but the development of environmental-friendly and cost-effective synthetic methods still faces challenges. The widely-used synthetic strategies generally involve molecular and particulate processing in vacuum or in liquid medium, which however, are capital intensive and are inefficient in materials and energy use.[1,2] Furthermore, many methods for semiconductor nanoparticles preparation require highly toxic solvents, explosive precursors, high temperature, and thus are not eco-friendly. To develop clean, nontoxic, and environmentally benign manufacturing procedures, biosynthesis provides a promising alternative because a number of microorganisms are capable of producing metal-containing nanoparticles in nature.[1,2] For example, a yeast *Torulopsis sp* is capable of producing PbS nanocrystals intracellularly when challenged with Pb^{2+}. Crystallites extracted from the biomass exhibit a sharp absorbance at 330 nm and are 2–5 nm in size.[3]

Among the wide variety of nanoparticles, we were interested in cadmium sulfide (CdS) nanoparticles as they have captured enormous attention as a semiconductor material in diverse applications such as fluorescent labels[4] and optoelectronic transistor components.[5] It has been reported that two yeast species, *Candida glabrata* and *Schizosaccharomyces pombe* (*S. pombe*), produce CdS nanoparticles when cultured in the presence of cadmium salts.[6–8] Such biosynthesis is attributed to the function of metal-chelating peptides glutathione (GSH) and phytochelatins (PCs). In the presence of heavy metal (e.g., Cd) stress, yeast cells increase the cellular pools of GSH (γ-Glu-Cys-Gly) and PCs ($(\gamma\text{-Glu-Cys})_n$-Gly, $n = 2–6$) which are synthesized from GSH in a heavy metal-dependent reaction.[9] GSH chelates the free metal ions and

Correspondence concerning this article should be addressed to Y.-C. Hu at yuchen@che.nthu.edu.tw or H.-C. Liang at HCLiang@itri.org.tw

Table 1. Primer Sequences for PCR

Primer	Gene	Sequence
P1	*gshA*-F (*Nde*I)	5′-gaggtccatatgatcccggacgtatcaca
P2	*gshA*-R (*Nde*I)	5′-ttctcatatgtcaggcgtgtttttccagccacacg
P3	*gshB*-F (*Nde*I)	5′-ggagaagacatatgatcaagctcggcatcg
P4	*gshB*-R (*Nde*I)	5′-aaggcatatgttactgctgctgtaaacgtgcttc
P5	pSE380-1F	5′-gtgcactctcagtacaatct
P6	pSE380-1R	5′-cggtgtgaaataccgcacag
P7	pSE380-2F	5′-ggtcgtatacagacaaaggacacactttaac
P8	pSE380-2R	5′-actggtgcagcaccttacgga

subsequently donates them to metal-sequestering PCs.[9] The formation of metal thiolate complex neutralizes the toxicity of Cd^{2+} ions and traps them inside the cells. Sulfide anions are readily incorporated into these complexes, resulting in the formation of CdS nanocrystals. CdS nanoparticles produced from *S. pombe* have a diameter of ≈2 nm and exhibit optical and electric properties that can be harnessed for the fabrication of diodes.[10]

Besides yeasts, procaryotic bacterium *Clostridium thermoaceticum* precipitates CdS on the cell surface and in the medium from cadmium chloride ($CdCl_2$) if cysteine hydrochloride is present in the growth medium.[11] Recently, intracellular biosynthesis of CdS nanoparticles is also demonstrated in *Escherichia coli* (*E. coli*) ABLE C and Tg1 strains when the cells are incubated with $CdCl_2$ and sodium sulfide (Na_2S).[12] CdS nanoparticle formation hinges dramatically on the growth phase of *E. coli* and is at least 20-fold higher in the cells in stationary phase than those in late-exponential phase, and nanoparticles are not detected in mid-exponential phase cells. However, the genetic and molecular basis of CdS formation in *E. coli* remains to be elucidated.

GSH is a ubiquitous tripeptide consisting of glutamate, cysteine, and glycine, and is the most abundant intracellular nonprotein thiol compound.[13] GSH is consumed in the detoxification of heavy metal and xenobiotics[14] and is a very efficient free radical scavenger. Intracellular GSH content is regulated by its continued turnover and its de novo synthesis depends on enzyme activities and cysteine availability.[15] Intracellular synthesis of GSH requires ATP and involves a two-step reaction whereby γ-glutamycysteine synthetase (γ-GCS) first catalyzes the reaction of cysteine and glutamate to form γ-glutamylcysteine. Following this step, glycine is ligated to γ-glutamycysteine to form GSH in a reaction catalyzed by gluthathione synthetase (GS). In *E. coli*, γ-GCS and GS are encoded by the genes *gshA* and *gshB*, respectively, and γ-GCS over-expression increases the GSH production in *E. coli*[16] and *Saccharmyces cerevisiae*.[17] Additionally, over-expression of GS in Indian mustard enhances its cadmium accumulation and tolerance.[15]

Owing to the pivotal role of GSH in heavy metal tolerance and CdS formation in yeasts, as well as the requirement of γ-GCS and GS for GSH synthesis, we surmised that over-expression of *gshA* or *gshB* in *E. coli* may increase the corresponding enzyme activities and enhance GSH synthesis, which in turn, may elevate the CdS nanoparticle formation. To test this hypothesis, two recombinant plasmids encoding *gshA* or *gshB* were constructed and transformed into *E. coli* ABLE C separately. Our data indicated that GS over-expression in *E. coli* augmented the intracellular content of GSH and hence improved the production of CdS nanoparticles, thus implicating the potential of genetic engineering approach for microbial biosynthesis of nanoparticles.

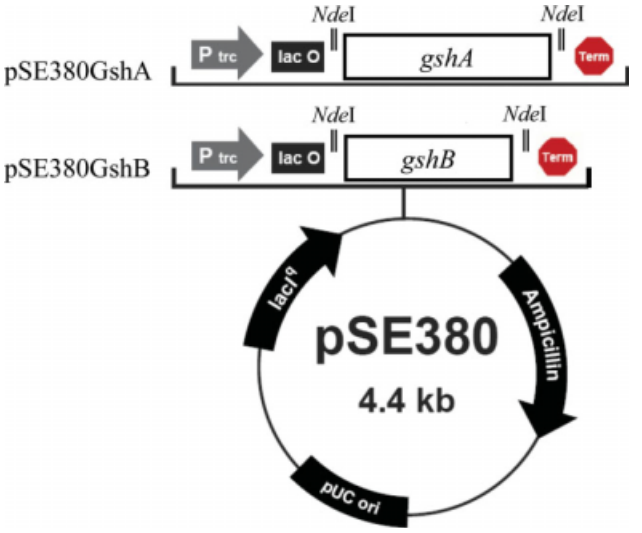

Figure 1. Schematic illustration of plasmids pSE380GshA and pSE380GshB.

The genes were flanked by *Nde*I sites and under the transcriptional control of *trc* promoter so that gene expression was induced by IPTG. Term denotes the transcription termination sequence and Lac O denotes the lac operator.

Materials and Methods

Construction of recombinant plasmids and cells

The *gshA* and *gshB* genes flanked by *Nde*I sites were amplified by polymerase chain reaction (PCR) from *E. coli* Tg1 (Strategene) using primers P1, P2, P3, and P4 (Table 1). The PCR products were subcloned into a TA-based cloning vector using the T&A cloning vector kit (Real Biotech Corp, Taiwan) to generate plasmids pTA-gshA and pTA-gshB. For protein expression, the expression vector pSE380 (Invitrogen) was chosen. Because the original *Nco*I site (ccatgg) in pSE380 possessed the start codon that could result in the expression of recombinant proteins with point mutation, the *Nco*I site in pSE380 was modified to the *Nde*I (catatg) site in two stages. First, the *Nde*I site located outside the multiple cloning site of pSE380 (nucleotides 2999–3004) was deleted via PCR-based site-directed mutagenesis. The PCR was performed using synthetic primers P5 and P6 (Table 1) and pSE380 as the template, followed by ligation of the amplicon (4.4 kb). Second, the *Nco*I site downstream of the *trc* promoter was changed to *Nde*I site by PCR using synthetic primers P7 and P8 (Table 1) and the ligated plasmid as the template. The amplicon (4.4 kb) was then ligated to form the modified pSE380 plasmid. The final recombinant expression plasmids, pSE380GshA and pSE380GshB (Figure 1), were constructed by individually subcloning the genes in pTA-gshA and pTA-gshB into the *Nde*I site in the modified pSE380, so that γ-GCS and GS expression was transcriptionally controlled by the *trc* promoter and inducible by IPTG (isopropyl-β-D-thiogalactopyranoside). The size, orientation, and sequence of *gshA* or *gshB* in the recombinant plasmids were confirmed by PCR, restriction enzyme digestion and sequencing (data not shown), respectively. These plasmids were transformed into *E. coli* ABLE C (Strategene) by standard calcium chloride transformation method for expression and CdS nanoparticle production.

Cell growth and induction

E. coli ABLE C harboring either pSE380GshA or pSE380GshB was selected following standard molecular

cloning techniques, resuspended in Luria-Bertani (LB) medium (Difco), plated onto agar plates containing LB medium and 100 μg/mL ampicillin, and cultivated at 37°C overnight. Colonies were picked, inoculated into 15 mL round-bottomed culture tubes containing 3-mL LB medium, and cultivated with rotation (50 rpm) at 37°C for 12 h. After the enrichment step, 0.5-mL broth was inoculated into 250 mL shake flasks containing 50-mL LB medium and cultivated with shaking (200 rpm) at 37°C. The cell growth was monitored by measuring the optical density at 600 nm (OD_{600}) throughout the culture. The expression of recombinant γ-GCS or GS was induced by adding IPTG at different final concentrations (1, 5, or 10 mM) when OD_{600} reached $\approx$0.5 at 3 h postinoculation.

Analysis of γ-GCS and GS expression by SDS-PAGE

After IPTG induction, the cells continued to be cultivated for another 13 h and were harvested. The cells were sonicated and centrifuged (13,000*g*, 10 min) to separate the cell lysate (supernatant) and cellular debris (pellet). Total protein concentrations in the lysate and the debris were measured by a protein assay kit (Bio-Rad Laboratories). Same amounts of proteins were loaded to 12% slab gels for sodium dodecyl sulfate-polyacrylamide gel electrophoresis (SDS-PAGE). The bands on the SDS-PAGE gels were scanned and quantified by scanning densitometry using Scion Image Shareware (Scion Corporation).

Quantification of GSH concentration

The GSH concentration was assayed in triplicate spectrophotometrically based on the reaction between GSH and 5,5′-dithiobis-2-nitrobenzoate (DTNB) as described.[18] In brief, the cells were cultivated as described earlier and induced by IPTG (1, 5, or 10 mM) at 3 h postseeding. Cysteine was added together with IPTG to the culture (final concentration = 1 mM) because cycteine is a limiting substrate for GSH synthesis and cysteine addition to the culture medium increases the GSH level in *Lactococcus lactis*.[19] The culture continued for another 13 h when stationary phase was reached. Wild-type cells were cultivated in an identical manner to serve as the control. A portion of the cells (24 mL) was washed by phosphate-buffered saline (PBS, pH 7.2), centrifuged, and then resuspended in 7.2-mL PBS. The cells were challenged with 0.8-mL $CdCl_2$ (final concentration = 1 mM) for 0, 20, 40, or 60 min to stimulate the GSH synthesis. Then the cells were centrifuged (12,000*g*, 20 min), resuspended in 8 mL ddH_2O, sonicated, and pelleted again. The lysate (200 μL) was mixed with 800-μL Tris buffer (0.1 M Tris-HCl, 1 mM EDTA, pH 8.0) and 25-μL dithioerythritol solution (2 mM) and incubated at room temperature. One hour later, 50-μL DTNB (10 mM, in 0.1 mM phosphate buffer, pH 7.5) was added to the mixture and the reaction continued for another 15 min. The absorbance of the reaction product 5 mercapto-2-nitrobenzoic acid was measured at 412 nm. The standard curve was generated using known amounts of GSH (Sigma) for the quantification.

Biosynthesis and analysis of CdS nanoparticles

Biosynthesis of CdS nanoparticles was performed as described earlier[12] with minor modifications. The cells were cultivated and induced as described earlier. Likewise, cysteine was supplemented to the medium at 3 h postinoculation to enhance GSH synthesis. The cells were cultivated for another 13 h and entered stationary phase. A portion of the cells (24 mL) was harvested, washed by PBS, resuspended in PBS, and challenged with $CdCl_2$ as described earlier. Twenty minutes later, 10 mM Na_2S was slowly added to the mixture to a final concentration of 1 mM, and the tube (protected from light) was rotated (20 rpm) at room temperature for CdS nanoparticles formation.

CdS nanoparticles were quantified indirectly by measuring the intracellular Cd concentration with an Inductively Coupled Plasma Optima Optical Emission Spectrometer (ICP, Kontron). At different time points following Na_2S addition, the cells were centrifuged and washed three times with PBS. The final wash buffer was analyzed by ICP to ensure that no residual Cd was present on the cell surface. The cells were then resuspended in 1-mL ddH_2O, lysed by sonication, and centrifuged again (12,000*g*, 20 min) to separate the pellet and the lysate. The concentrations of Cd in the lysate (ppm) were quantified by ICP and converted to milligram CdS per gram dry cell weight (mg/g DCW).

Transmission electron microscopy (TEM) and high resolution TEM (HRTEM)

CdS nanoparticles were produced as described earlier and characterized by transmission electron microscopy (TEM) and energy dispersive X-ray spectroscopy (EDS). The cells were harvested 90 min after Na_2S addition, washed with PBS three times, resuspended in ddH_2O, sonicated, and centrifuged (12,000*g*, 10 min) to separate the cellular debris and supernatant containing the CdS nanoparticles. TEM samples were prepared by floating ultra carbon film-coated copper grids (TED Pella) onto 5-μL CdS nanoparticle solution for 5 min. The excess solution on TEM grids was removed by filter paper, and the grids were dried in an oven at 60°C overnight. The samples were visualized with a low-resolution TEM (H-7500, Hitachi) operating at 120 KeV, or with a high-resolution TEM (HRTEM, JEM-2010, JEOL) operating at 200 KeV. The images were captured digitally with a Gatan DigitalMicrograph system. EDS was performed on the HRTEM (JEM-2010) equipped with a spectrometer (Link ISIS 300).

Statistical analysis

All quantitative data were analyzed using independent samples *t*-tests and are expressed as means $\pm$ standard deviations (SD) of three independent experiments. $P < 0.05$ was considered significant.

Results

Growth curves of recombinant cells and confirmation of protein expression

The recombinant plasmids (pSE380GshA and pSE380GshB) harboring *gshA* and *gshB* were constructed (Figure 1), and *E. coli* ABLE C was selected as the host cell as it was shown to be capable of CdS nanoparticle production.[12] To examine whether plasmid transformation and IPTG induction affected the cell growth, the cells harboring either pSE380GshA or pSE380GshB were induced with IPTG (1, 5, or 10 mM) at 3 h postinoculation and continued to be cultivated for another 13 h. The wild-type *E. coli* ABLE C cells were cultivated in parallel without IPTG induction

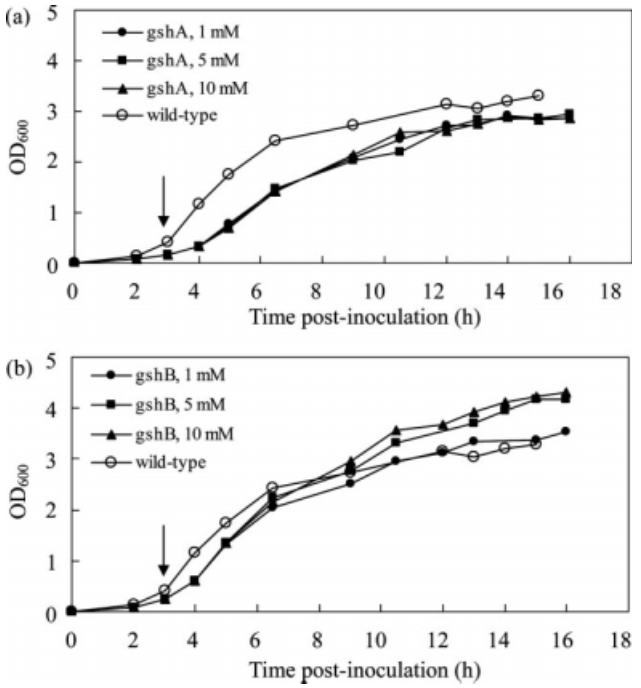

Figure 2. Effects of transformation and IPTG induction on cell growth.

The recombinant *E. coli* ABLE C harboring either pSE380GshA (a) or pSE380GshB (b) were inoculated into the shake flasks and induced with IPTG at 3 h postinoculation. The cells were sampled for OD_{600} measurements at different time points. Wild-type cells were cultivated in parallel as the control. Arrows indicate the induction timing.

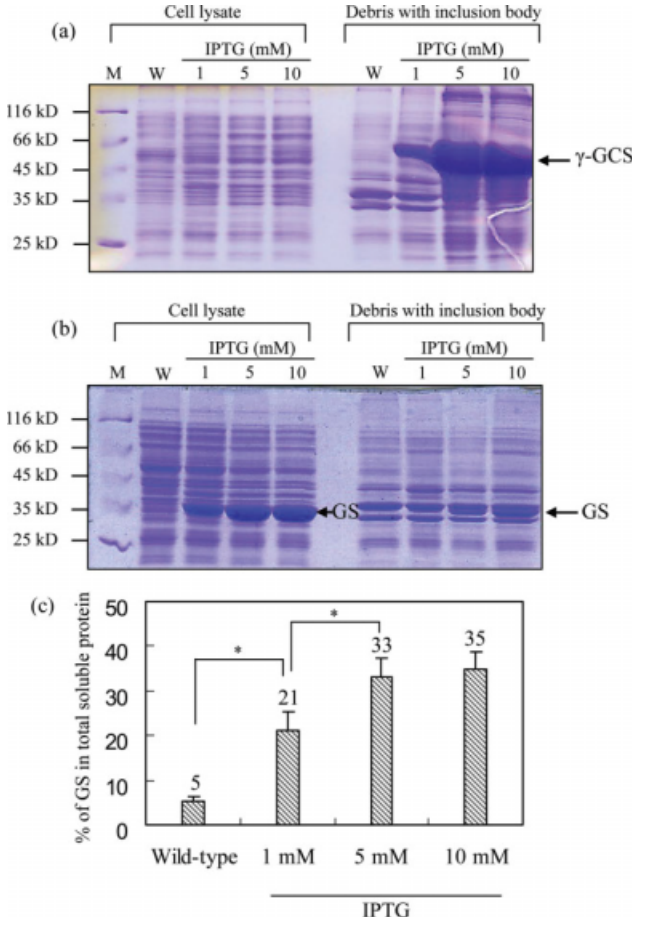

Figure 3. Analysis of γ-GCS and GS expression.

(a) SDS-PAGE analysis of the proteins from the pSE380GshA-transformed cells. (b) SDS-PAGE analysis of the proteins from the pSE380GshB-transformed cells. (c) The percentage of GS in the lysate of pSE380GshB-transformed cells as estimated by scanning densitometry. The cells were cultivated and induced with IPTG as in Fig. 2 and were harvested at 16 h postinoculation. Wild-type cells were cultivated in parallel as the control. The cell lysate and debris were separated by centrifugation and analyzed by SDS-PAGE. The data are representative of three independent culture experiments. M, molecular weight marker. W, wild-type cells. $*P < 0.05$.

and served as the control. When compared with the wild-type cells, Figure 2a unravels hampered cell growth upon IPTG induction of the cells carrying pSE380GshA even at an IPTG concentration as low as 1 mM. In contrast, IPTG induction of the cells harboring pSE380GshB did not negatively influence the cell growth (Figure 2b).

To confirm the expression of γ-GCS and GS, the cells were harvested at 16 h postinoculation and the cell lysate and debris containing inclusion bodies were analyzed by SDS-PAGE. As illustrated in Figure 3a, thick bands whose molecular mass corresponded to that of γ-GCS (≈55 kD) were detected in the debris of the pSE380GshA-transformed cells, but not in that of the wild-type cells; also the band intensity increased with the IPTG concentration, thereby confirming the γ-GCS expression. γ-GCS was barely detectable in the cell lysate, suggesting that γ-GCS over-expression primarily led to the formation of inclusion bodies. For the pSE380GshB-transformed cells (Figure 3b), raising the IPTG concentration overly elevated the expression of GS (≈35 kD) in the cell lysate but only minor bands indicative of GS were detectable in the debris, implying that IPTG induced the expression of GS that was mainly present in soluble form.

The percentages of soluble GS in the cell lysate were estimated by scanning densitometry of the SDS-PAGE gels. Figure 3c delineates that GS accounted for ≈5% of total soluble proteins in the wild-type cells, but induction of the pSE380GshB-transformed cells with 1 mM IPTG significantly increased the percentage to ≈21%, which further rose to ≈33% upon 5 mM IPTG induction. Increasing the IPTG concentration to 10 mM marginally elevated the percentage to ≈35%.

Enhanced synthesis of GSH and CdS nanoparticles in the cells over-expressing GS

Because γ-GCS over-expression gave rise to inclusion body formation and hindered cell growth, which were indicative of impaired cell physiology, all subsequent experiments were performed using the cells over-expressing GS. To explore whether GS over-expression augmented the GSH synthesis, the recombinant cells were cultivated and induced with IPTG as in Figure 3 and the cells were harvested at 16 h postinoculation when the cells entered stationary phase. This timing was chosen because the CdS nanoparticles formation in *E. coli* ABLE C occurred predominantly in the stationary phase.[12] GSH synthesis was stimulated by cell exposure to $CdCl_2$ which imparted the metal stress, and intracellular GSH concentrations were measured at different time points.

Immediately after $CdCl_2$ addition (0 min), the GSH concentrations in all groups were similar (Figure 4a) because GS is not rate limiting for GSH synthesis in the absence of heavy metals.[15] Without GS over-expression, the GSH concentration remained stable at ≈4 μmol/g DCW in the wild-type cells from 0–60 min presumably due to the continued

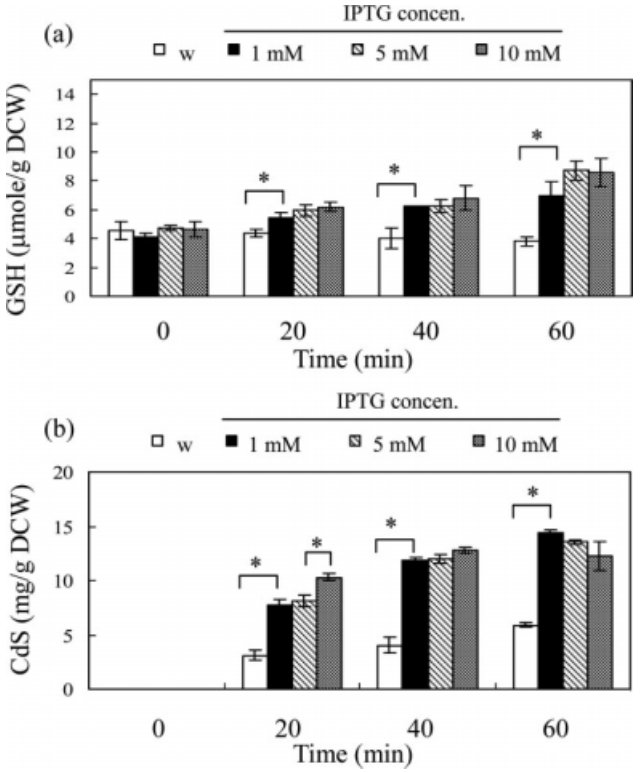

Figure 4. Effects of GS over-expression on the intracellular synthesis of GSH (a) and CdS nanoparticles (b).

The recombinant cells harboring pSE380GshA were cultivated and induced with IPTG. Note that at 3 h postinoculation cysteine was added to a final concentration of 1 mM. The cells were harvested at 16 h postinoculation and GSH synthesis was boosted by exposing the cells to $CdCl_2$ (final concentration = 1 mM). Intracellular GSH concentrations were measured at different time points after $CdCl_2$ challenge. The CdS production was triggered by sequential addition of $CdCl_2$ and Na_2S (final concentration = 1 mM) and was indirectly quantified by ICP at different time points after Na_2S addition. The original Cd concentrations in the sample (ppm) were converted to mg/g DCW. All data represent the averages ±SD of three independent culture experiments. *$P < 0.05$.

synthesis and consumption of GSH. In marked contrast, with GS over-expression the GSH concentration in the recombinant cells induced with 1 mM IPTG increased significantly ($P < 0.05$, when compared with the wild-type cells) to ≈5.5 μmol/g DCW in 20 min, and steadily increased to ≈7.0 μmol/g DCW in 60 min, confirming that GS over-expression elevated GSH synthesis upon exposure to $CdCl_2$. Increasing the IPTG concentration to 5 and 10 mM further increased the GSH concentrations to ≈8.7 and ≈8.6 μmol/g DCW, respectively, at 60 min postchallenge.

To correlate the GSH production and CdS formation, the cells were cultivated, induced with IPTG and challenged with $CdCl_2$ as in Figure 4a, but 20 min after $CdCl_2$ addition Na_2S was supplemented to stimulate the formation of CdS nanoparticles. Because no reliable methods for nanoparticle quantification are currently available, the amounts of intracellular CdS were indirectly quantified by ICP at different time postaddition as described.[12,20] Figure 4b confirms that the amount of intracellular CdS in all groups increased steadily with time. Strikingly, the recombinant cells produced significantly more ($P < 0.05$) CdS than the wild-type cells at as early as 20 min, at which time 10 mM IPTG resulted in the highest CdS production. Nevertheless, at the end point (60 min) the 1 mM IPTG group led to the most abundant CdS accumulation (≈14.4 mg/g DCW), which was

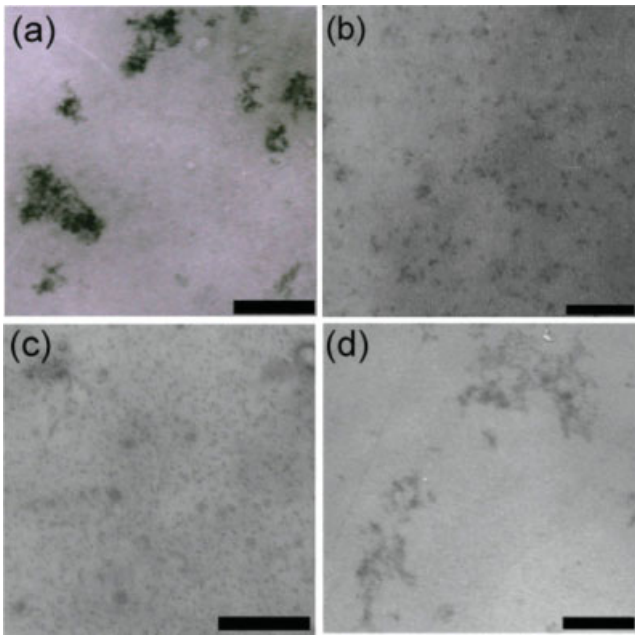

Figure 5. TEM images of CdS nanoparticles synthesized from *E coli* ABLE C.

(a) Wild-type; (b) recombinant cells induced with 1 mM IPTG; (c) recombinant cells induced with 5 mM IPTG; (d) recombinant cells induced with 10 mM IPTG. Images are representative of the particles produced from three independent culture experiments. Bar, 100 nm.

≈2.5 times that of the control (≈5.9 mg/DCW) at 60 min. Figures 4a,b collectively demonstrate that GS over-expression concurred with the elevated GSH synthesis and intracellular CdS accumulation, but exceedingly high GSH synthesis (e.g., induction with 5 or 10 mM IPTG) did not proportionally improve the CdS accumulation.

Characterization of CdS nanoparticles produced from the recombinant E. coli

The CdS nanoparticles were synthesized and extracted as described in Materials and Methods and characterized by TEM. It should be noted that the samples were not negatively stained, thus only electron-dense particles (e.g., CdS) were observable. The TEM images revealed particles of similar size derived from all groups, regardless of IPTG concentrations. Intriguingly, nanoparticles from the wild-type cells had a higher propensity to aggregate as huge nanoparticle clusters (Figure 5a), whereas the particles from the recombinant cells appeared to exhibit better dispersion as fewer aggregates were observed (Figures 5b–d). However, no difference in dispersibility was observed between the CdS nanoparticles produced from different IPTG groups.

CdS nanoparticles from the wild-type (Figure 6a) and recombinant cells induced with 1 mM IPTG (Figure 6b) were further characterized by HRTEM, which confirmed that the CdS nanoparticles exhibited single crystal structures. The 2.9 nm CdS nanoparticle (indicated by the arrow in Figure 6b) had a d spacing of 0.332 nm, corresponding to the (002) plane in wurtize CdS. The fast fourier transforms (FFTs) obtained from the fields of particles (the insets of Figures 6a,b) revealed rings corresponding to the *d* spacing of 0.357 nm and 0.333 nm which can be indexed to the (100) and (002) lattice planes in wurtize CdS, respectively. These data altogether confirmed the wurtize nature of the particles.

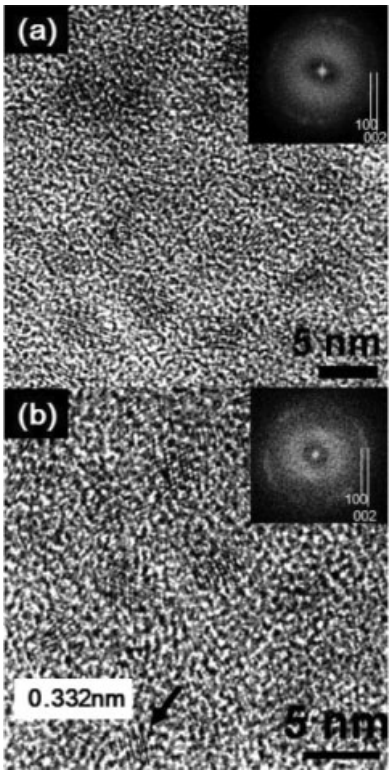

Figure 6. HRTEM images of CdS nanoparticles synthesized from *E. coli* ABLE C.

(a) Wild-type cells; (b) recombinant cells induced with 1 mM IPTG. The FFTs (insets of (a) and (b)) were obtained from the corresponding TEM images, and the *d* spacings of the two rings in the FFTs (0.357 and 0.333 nm) agreed with the reference values (0.359 and 0.336 nm) for wurtize CdS (100) and (002), respectively. The lattice spacing of 0.332 nm of a nanoparticle indicated by the arrow corresponded to the (002) plane of wurtize CdS.

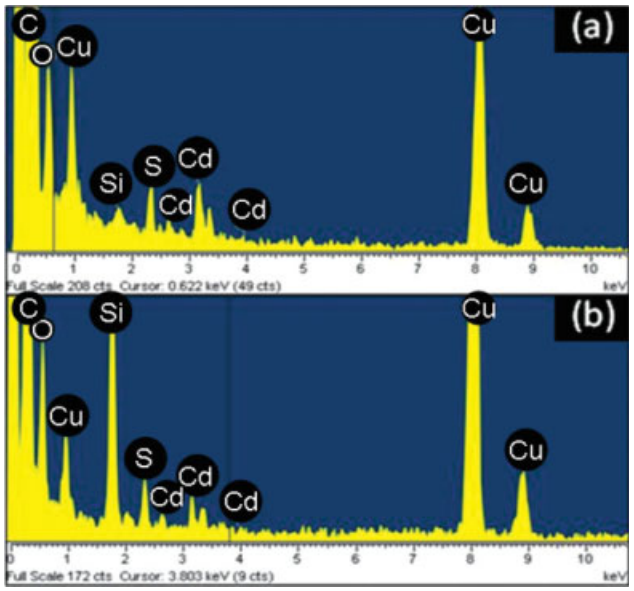

Figure 7. EDS spectrums obtained from CdS nanoparticles imaged by TEM as shown in Figure 6a (a) and Figure 6b (b), respectively.

The C and O peaks resulted from the cell lysates while C, Cu, and Si signals possibly originated from the carbon film-coated copper TEM grid.

Table 2. The Ratio of Cd/S in the Particles Produced from the Wild-Type and Recombinant Cells

	Wild-Type		1 mM IPTG Group	
Element	Weight%	Atomic%	Weight%	Atomic%
S	21.00	48.23	27.75	57.38
Cd	79.00	51.77	72.25	42.62
Cd/S		1.07		0.74

The energy dispersive X-ray spectrum (EDS) obtained from the fields of nanoparticles (Figure 6) also attested the presence of Cd and S in the particles extracted from the wild-type (Figure 7a) and recombinant cells (Figure 7b). Because the samples were not purified, other noise signals in the EDS presumably stemmed from the cellular components (e.g., C and O) or from the TEM grids (e.g., C, Cu, and Si). The atomic ratio of Cd/S in the particles from the wild-type cells was 1.07 (Table 2), which accurately corresponded to the elemental composition of Cd and S in the CdS particles. Conversely, the Cd/S ratio in the particles from the recombinant cells was 0.74.

Discussion

Glutathione (GSH) is an important antioxidant tripeptide in living cells against oxidative stress and also plays a key role in CdS nanocrystals synthesis in yeasts.[21] As such, the overriding objective of this study was to genetically engineer *E. coli* ABLE C, a bacterium recently shown to allow for CdS nanoparticle formation,[12] hoping that the over-expression of γ-GCS or GS leads to CdS nanoparticles over-production. Although no Western blot analyses were performed due to the lack of cognate antibodies, Figures 2 and 3 collectively indicated that IPTG induction of *E. coli* ABLE C harboring pSE380GshA led to the expression of γ-GCS in the form of inclusion body and impaired the cell growth, whereas IPTG induction of the recombinant cells harboring pSE380GshB gave rise to abundant expression of GS in soluble form and barely impeded the cell growth.

Furthermore, GS over-expression in the recombinant cells paralleled the elevated GSH synthesis (Figure 4a) and hence the increased production of CdS nanoparticles (Figure 4b) after addition of $CdCl_2$ and Na_2S. It should be emphasized that although ICP indirectly measured the intracellular Cd content rather than directly quantified the CdS particles, Cd is not normally present inside the cells hence the intracellular accumulation of Cd was indicative of CdS particle formation. The maximum yield of CdS nanoparticles attained by 1 mM IPTG induction reached 14.4 mg/g DCW, which not only was $\approx$2.5 times that of the wild-type *E. coli* ABLE C (5.9 mg/g DCW) but also considerably exceeded the yield achieved by *S. pombe* ($\approx$1.4 mg/g DCW).[10] Nevertheless, induction with higher IPTG concentrations (e.g., 5 and 10 mM) and the ensuing elevated GS over-expression and GSH synthesis did not further improve the production levels of CdS nanoparticles (Figures 3 and 4), suggesting that over a threshold GSH concentration other factors (e.g., the availability and feeding strategy of $CdCl_2$ and Na_2S precursors, etc.) restricted the CdS production.

Importantly, the resultant particles resembled the CdS nanoparticles produced from the wild-type cells in size (2–5 nm, Figures 5 and 6) and the hexagonal wurtzite lattice structures (Figure 6), which concurred with the size and crystal structure of CdS nanoparticles synthesized from the wild-type *E. coli* ABLE C as reported earlier.[12] Yet it was

intriguing that the CdS nanoparticles from the recombinant cells exhibited better dispersibility and contained a higher fraction of S than Cd, when compared with those from the wild-type cells (Figure 7 and Table 2). Because CdS nanoparticles synthesized in microorganisms are capped with short peptides such as GSH or PC[21,24] and the amount of GSH capped to CdS nanoparticles influences the particle properties,[21] the discrepancy in dispersibility and elemental composition presumably originated from the enhanced GSH production and surface coating of GSH and/or PC on the nanoparticle in the recombinant cells. Further characterization of the particle properties and investigations of this hypothesis are underway.

Conclusions

In summary, we have shown that GS over-expression in *E. coli* ABLE C in conjunction with metal stress simultaneously enhance the biosynthesis of intracellular GSH and CdS nanoparticles, and induction with 1 mM IPTG is sufficient to elevate the yield of CdS nanoparticles considerably when compared with the wild-type cells. These data implicate the potential of genetic engineering approach to enhancing the CdS nanoparticle biosynthesis in bacteria and unravel the importance of GS and GSH in this process. Although biosynthesis of CdS nanoparticles has been demonstrated in other microorganisms, our approach is advantageous not only in the improved yield but also in that industrial-scale bioprocess of *E. coli* fermentation has been well established, hence future mass production is simple. As opposed to chemical synthesis processes which require high temperature and toxic organic solvents, *E. coli*-based biosynthesis is conducted at 37°C and obviates the need of toxic solvents, thus representing a more energy-efficient and eco-friendly method alternative to chemical synthesis. At present, this study aims to explore the feasibility of using genetic engineering techniques for CdS nanoparticle over-production and subsequent process optimization to improve the yield is needed. Because the yield and properties are critically dependent on cell physiology and availability of precursors (e.g., cysteine, $CdCl_2$ and Na_2S), process optimization may be performed by adjusting the cultivation method (e.g., altering medium formulation and induction timing), changing precursor concentration and feeding strategy, or further engineering the intracellular CdS processing pathway. As GSH also forms complexes with Zn^{2+} and Pb^{2+},[21] this genetic engineering approach may also be extended to the over-production of other semiconductor nanoparticles including PbS and ZnS.

Acknowledgments

The authors gratefully acknowledge the financial support from the National Tsing Hua University Booster Program (96N2511E1), CGMH-NTHU Joint Research Program (CGTH96-T8 and CMRPG361041), and National Science Council (NSC 96-2627-B-007-018), Taiwan.

Literature Cited

1. Klaus-Joerger T, Joerger R, Olsson E, Granqvist C-G. Bacteria as workers in the living factory: metal accumulating bacteria and their potential for materials science. *Trends Biotechnol*. 2001;19:15–20.
2. Mandal D, Bolander ME, Mukhopadhyay D, Sarkar G, Mukherjee P. The use of microorganisms for the formation of metal nanoparticles and their application. *Appl Microbiol Biotechnol*. 2006;69:485–492.
3. Kowshik M, Vogel W, Urban J, Kulkarni SK, Paknikar KM. Microbial synthesis of semiconductor Pbs nanocrystallites. *Adv Mater*. 2002;14:815–818.
4. Jaiswal JK, Mattoussi H, Mauro JM, Simon SM. Long-term multiple color imaging of live cells using quantum dot bioconjugates. *Nat Biotechnol*. 2003;27:47–51.
5. Brown KR, Lidar DA, Whaley KB. Quantum computing with quantum dots on quantum linear supports. *Phys Rev A*. 2002; 65:012307-1-19.
6. Krumov N, Oder S, Perner-Nochta I, Angelov A, Posten C. Accumulation of Cds nanoparticles by yeasts in a fed-batch bioprocess. *J Biotechnol*. 2007;132:481–486.
7. Dameron CT, Smith BR, Winge DR. Glutathione-coated cadmium-sulfide crystallites in *Candida Glabrata*. *J Biol Chem*. 1989;264:17355–17360.
8. Dameron CT, Reese RN, Mehra RK, Kortan AR, Carroll PJ, Steigerwald ML, Brus LE, Winge DR. Biosynthesis of cadmium-sulfide quantum semiconductor crystallites. *Nature*. 1989;338: 596–597.
9. Mendoza-Cózatl D, Loza-Tavera H, Hernández-Navarro A, Moreno-Sánchez R. Sulfur assimilation and glutathione metabolism under cadmium stress in yeast, protists and plants. *FEMS Microbiol Rev*. 2005;29:653–671.
10. Kowshik M, Deshmukh N, Vogel W, Urban J, Kulkarni SK, Paknikar KM. Microbial synthesis of semiconductor Cds nanoparticles, their characterization, and their use in the fabrication of an ideal diode. *Biotechnol Bioeng*. 2002;78:583–588.
11. Cunningham DP, Lundie LL Jr. Precipitation of Cadmium by *Clostridium Thermoaceticum*. *Appl Environ Microbiol*. 1993;59: 7–14.
12. Sweeney RY, Mao C, Gao X, Burt JL, Belcher AM, Georgiou G, Iverson BL. Bacterial biosynthesis of cadmium sulfide nanocrystals. *Chem Biol*. 2004;11:1553–1559.
13. Li Y, Wei G, Chen J. Glutathione: a review on biotechnological production. *Appl Microbiol Biotechnol*. 2004;66:233–242.
14. Coblenz A, Wolf K. The role of glutathione biosynthesis in heavy metal resistance in the fission yeast *Schizosaccharomyces Pombe*. *FEMS Microbiol Rev*. 1994;14:303–308.
15. Zhu YL, Pilon-Smits EA, Tarun AS, Weber SU, Jouanin L, Terry N. Cadmium tolerance and accumulation in indian mustard is enhanced by overexpressing gamma-glutamylcysteine synthetase. *Plant Physiol*. 1999;121:1169–1178.
16. Murata K, Kimura A. Cloning of a gene responsible for the biosynthesis of glutathione in *Escherichia Coli* B. *Appl Environ Microbiol*. 1982;44:1444–1448.
17. Fan X, He X, Guo X, Qu N, Wang C, Zhang B. Increasing glutathione formation by functional expression of the gamma-glutamylcysteine synthetase gene in *Saccharomyces Cerevisiae*. *Biotechnol Lett*. 2004;26:415–417.
18. Anderson ME. Determination of glutathione and glutathione sulfide in biological samples. *Methods Enzymol*. 1985;113:548–555.
19. Li Y, Hugenholtz J, Sybesma W, Abee T, Molenaar D. Using *Lactococcus Lactis* for glutathione overproduction. *Appl Microbiol Biotechnol*. 2005;67:83–90.
20. Lima AIG, Corticeiro SC, Figueira E. Glutathione-mediated cadmium sequestration in *Rhizobium Leguminosarum*. *Enzyme Microb. Technol*. 2006;39:763–769.
21. Bae W, Mehra RK. Properties of glutathione- and phytochelatin-capped Cds bionanocrystallites. *J Inorg Biochem*. 1998;69:33–43.
22. Hatcher EL, Chen Y, Kang YJ. Cadmium resistance in A549 cells correlates with elevated glutathione content but not antioxidant enzymatic activities. *Free Radic Biol Med*. 1995;19:805–812.

Manuscript received July 24, 2008, and revision received Nov. 17, 2008.